A THEORETICAL DISCUSSION ON SOME ASPECTS OF ATOMIC FLUORESCENCE SPECTROSCOPY IN FLAMES

C. TH. J. ALKEMADE
Fysisch Laboratorium, Rijks-Universiteit Utrecht, The Netherlands

ABSTRACT

In Section 1 a general theoretical expression is derived for the gain in signal strength attainable by atomic fluorescence spectroscopy (AFS) when compared to flame emission spectroscopy (FES), if the same atomic line, flame and measuring instrument are used. In particular, the usefulness of the hot hydrogen–oxygen flame in AFS is discussed. In Section 2 the shape of the analytical curve in AFS is derived from the curve-of-growth theory, for a continuum as well as a narrow-line source and under idealized conditions. The effects of partial illumination of the observed flame cell, and of partial observation of the illuminated flame cell on the shape of this curve, are shown both theoretically and experimentally. Possible sources of deviation of practical curves from the calculated curves are mentioned. In Section 3 the advantages of non-resonance fluorescence are summarized. A general theoretical expression is derived for the ratio of fluorescence signals obtained when one or another atomic line is used as an exciting and fluorescent line, respectively. This is done for direct line fluorescence as well as stepwise line fluorescence.

1. COMPARISON OF SIGNAL STRENGTHS ATTAINABLE IN ATOMIC FLUORESCENCE (AFS) AND FLAME EMISSION SPECTROSCOPY (FES)

The improvement of detection limits is one of the main goals in AFS. The actual detection limit depends on many factors and will vary strongly from element to element and from instrument to instrument. Elaborate theoretical expressions based on detailed noise considerations have been given in the literature[1,2]. These expressions are difficult to survey and do not demonstrate clearly the fundamental advantages of AFS over FES in this respect. Assuming idealized conditions we shall briefly derive a simple expression for the fluorescence signal compared to the thermal emission signal, leaving out all accidental factors. Only a few fundamental parameters will be retained that enable us to estimate roughly the gain in detection limit attainable by AFS. The derivation of the gain factor to be presented makes use of some general relationships only and bypasses in a way the detailed and elaborate calculations of absolute detection limits.

In comparing the two spectroscopic methods, we assume that the same atomic resonance line is excited and observed in the same flame volume fed by the same sprayer. Also, the solid angle under which the flame is observed,

the spectral apparatus and the photometer are assumed to be identical in the two cases. We suppose that in both cases the detection limit is set by the common shot-noise level due to the flame-background signal. When this shot-noise is not detectable because of a very low background emission, the detection limit may be supposed to be set by the dark-current and amplifier noise. These noise effects will again be the same in AFS and FES, when the same photometer is used. We disregard the contribution of scattering to the background noise in AFS, since this noise source is accidental and may be overcome by appropriate instrumental measures. Under these conditions, the ratio of the detection limits attainable with the two spectroscopic methods is determined only by the ratio of the absolute signal strengths. When the exciting light-beam or the flame emission is chopped by a light-modulator, an additional factor $\sqrt{2}$ may occur in the ratio of the detection limits. This small effect will be disregarded here. For simplicity's sake, the temperature T_f and composition of the flame part under observation is assumed to be homogeneous. The same applies to the radiation density ρ^s (in erg cm^{-3}) or the spectral radiation density ρ^s_λ (in erg cm^{-3} per unit of wavelength interval in Å) of the exciting light-beam throughout the observed flame part. Since we are just comparing detection limits, the weakening of the exciting light-beam due to its absorption in the flame, as well as the self-absorption of the (re-)emitted atomic radiation may be neglected. In other words, our calculations are applicable in good approximation for sufficiently small metal concentrations n (number of atoms per cm^3). In this case the following calculations are also valid when the distribution of atoms is not homogeneous.

(a) Case of continuum source

The concentration of excited atoms in the case of a Boltzmann equilibrium is denoted by $n^\star_{th}$†. In the presence of a continuum radiation field with spectral density of $\rho^s_{\lambda_0}$ at line centre λ_0, the concentration will be raised to a higher value $n^\star$. The fluorescence radiation intensity (expressed in number of photons re-emitted in all directions per cubic centimetre and per second) is given by the product: $A(n^\star - n^\star_{th})$, where A is the optical transition probability (per second). This product is also equal to the number of excitations, U, per second and per cubic centimetre by absorption of primary photons, multiplied by the yield factor Y of resonance fluorescence. This factor is defined as the fraction of photons absorbed that are re-emitted as fluorescence in the limit of negligible self-absorption. Thus we have (see also footnote†)

$$A(n^\star - n^\star_{th}) = UY \tag{1}$$

† In actual flames (without external light-source) the excited-state population at low atom concentrations will be lower than the Boltzmann value, because the rate of radiative de-excitation is not compensated by an equal rate of photo-excitation. Exact compensation exists only if the radiation density equals the Planck value at the flame temperature. The relative deviation from the Boltzmann population is equal to the fluorescence yield factor Y defined by equation 2, in the limit of vanishing atom concentrations[2–4]. In normal flames used in FES, Y amounts to a few per cent only, so we may still regard $n^\star_{th}$ as a good measure for the signal strength in FES. In flames used in AFS, Y may be as large as about a half, and $n^\star_{th}$ in equation 1 should properly be replaced by $n^\star_{th}(1 - Y)$. For simplicity's sake the factor $(1 - Y)$ is omitted in the following derivation. An exact derivation has been given[5].

with

$$Y = A/(A + k) \tag{2}$$

Herein k denotes the probability per second that an excited atom is deactivated by a quenching collision.

If, in principle, we could place the flame inside a black box with the same temperature as the flame, thermodynamic equilibrium would be fully attained. A detailed balance could then be applied to the rates of photon absorption and photon emission, respectively, which yields the relation

$$An_{th}^{\star} = U_{th} \tag{3}$$

Here U_{th} is the rate of photon absorption inside the black box where the spectral radiation density is equal to the Planck density, $\rho_{\lambda_0}^{b}(T_f)$, at flame temperature. Dividing the corresponding sides of equations 1 and 3 we get

$$(n^{\star} - n_{th}^{\star})/n_{th}^{\star} = YU/U_{th} \tag{4}$$

Since the absorption coefficient of the atomic vapour is not influenced by the presence of a radiation field, we expect U/U_{th} simply to be equal to the corresponding ratio of spectral densities, $\rho_{\lambda_0}^{s}/\rho_{\lambda_0}^{b}(T_f)$, Thus we get from equation 4

$$(n^{\star} - n_{th}^{\star})/n_{th}^{\star} = Y\rho_{\lambda_0}^{s}/\rho_{\lambda_0}^{b}(T_f) \tag{5}$$

When a continuum source with spectral radiance $B_{\lambda_0}^{s}$ (denoting power emitted per square centimetre, per sterad and per unit wavelength interval) is imaged on the observed part of the flame under a solid angle Ω, the spectral irradiance E_{λ_0} (i.e. the power received by the flame surface per square centimetre and per unit wavelength interval) is, at its maximum, equal to $B_{\lambda_0}^{s}\Omega$. Introducing formally the radiance temperature T_s of the continuum source at λ_0 by the relation: $B_{\lambda_0}^{b}(T_s) \equiv B_{\lambda_0}^{s}$, the maximum irradiance received by the flame can also be written as: $B_{\lambda_0}^{b}(T_s)\Omega$. In fact T_s is the temperature of a black body that has the same radiance (given by the Planck law) as the actual source at λ_0.

When Ω equals its maximum value 4π sterad, the flame would effectively be surrounded by a black body at temperature T_s and the spectral radiation density would equal the Planck value $\rho_{\lambda_0}^{b}(T_s)$. When the experimental conditions are such that $\Omega < 4\pi$ as is usual, the (maximum) spectral density attainable in the flame by the use of the continuum source considered amounts to $(\Omega/4\pi)\rho_{\lambda_0}^{b}(T_s)$. Substituting the latter value for $\rho_{\lambda_0}^{s}$ in equation 5, we find that the maximum of the ratio $(n^{\star} - n_{th}^{\star})/n_{th}^{\star}$ attainable under the stated conditions is

$$(n^{\star} - n_{th}^{\star})/n_{th}^{\star} = Y(\Omega/4\pi)\{\rho_{\lambda_0}^{b}(T_s)/\rho_{\lambda_0}^{b}(T_f)\} \tag{6}$$

Under the simplifying assumptions made earlier in this Section, this ratio of excited atom concentrations yields directly the ratio of fluorescence to thermal emission signals. Again, this equals the gain in detection limit that is attainable — under the assumed experimental conditions—by the application of AFS. It appears that the only parameters of the atomic resonance line involved in this gain are its wavelength λ_0 and the yield factor Y.

It is interesting to note that neither the transition probability A nor the (integrated) absorption coefficient occurs explicitly in the RHS of equation 6. Of course, A is implicitly contained in Y (see equation 2), but flame conditions might, in principle, be chosen such that $Y \approx 1$, so that Y becomes virtually independent of A. The independence of the gain factor of the emission and absorption properties of the atoms concerned (for $Y \approx 1$) is based on the proportional relationship that fundamentally exists between A and the integrated absorption coefficient[6]. When both quantities are raised by the same factor, the rates of the radiative de-excitation and excitation processes (for given $\rho^s_{\lambda_0}$ and for $Y \approx 1$) again hold each other in balance, and the value of $n^\star$ will not be changed.

The only parameter of the continuum source involved in equation 6 is its radiance temperature T_s (which may depend on λ_0 when the source is not 'optically black'). The parameters Y and T_f depend on the flame chosen, while Ω is determined by the optical components. As expected, the gain in the detection limit is proportional to Y, which may vary from a few per cent in flames diluted by nitrogen, to above 50 per cent in premixed hydrogen–oxygen flames diluted by argon[2, 3, 7, 8]. Realistic values of Ω may range approximately from 0·1 to 1 sterad; the use of a mirror behind the flame may nearly double the effective solid angle. So at best we can expect $Y\Omega/4\pi$ to be roughly 0·05. Any substantial gain in the detection limit must thus come from the ratio of the Planck factors. This ratio may be very large for ultra-violet lines, when T_s and T_f differ by some thousands of °K.

If we take, for example, $T_f = 2000$°K, $Y = 0{\cdot}5$, $\Omega = 1$ sterad and $\lambda_0 = 3000$ Å, we calculate from equation 6 a theoretical gain in the detection limit of the order of 10^6, if a xenon arc with radiance temperature $T_s \approx 6000$°K is used. When T_f is increased to 3000°K, the gain is lowered by a factor of 3×10^3, but is still very large.

Of course, when discussing practical detection limits, we should consider many other factors too. For example, the optimum choice of analysis line and flame temperatures may be different in AFS and FES. The flame background fluctuations as observed in FES may exceed the shot-noise level. On the other hand, the application of FES may allow one to observe a larger flame volume than could be illuminated by the light-source in AFS because of the limited extensions of the source etc. It was not our intention to discuss these additional, practical factors which may sensibly vary from case to case. The simple expressions derived only serve as a first guide to give a rough insight into the essential parameters that determine the performance of AFS when compared to FES.

(b) Case of sharp-line source

The theoretical gain in the detection limit attainable by AFS with a sharp-line source can be found from equation 5, if we replace $\rho^s_{\lambda_0}$ therein by the effective spectral density $\rho^s/\Delta\lambda_{\text{eff.}}$ of the exciting light-beam in the flame

$$(n^\star - n^\star_{th})/n^\star_{th} = Y(\rho^s/\Delta\lambda_{\text{eff.}})/\rho^b_{\lambda_0}(T_f) \qquad (7)$$

Here ρ^s (erg/cm^3) is the radiation density integrated over the whole spectral width of the exciting line, which is supposed to be small compared to the

effective width $\Delta\lambda_{\text{eff.}}$ of the absorption line. The latter quantity is defined by

$$\Delta\lambda_{\text{eff.}} = \int k(\lambda)\,\mathrm{d}\lambda / k(\lambda_0)$$

where $k(\lambda)$ is the wavelength-dependent absorption coefficient and the integration is taken over the whole width of the absorption line. An exact derivation has been given by Alkemade and Zeegers[5]. The only atomic line parameters involved in equation 7 are λ_0, $\Delta\lambda_{\text{eff.}}$ and Y. The properties of the light-source and of the optical system that images this source in the flame are contained in ρ^s, while T_f, Y and $\Delta\lambda_{\text{eff.}}$ still depend on the kind of flame chosen.

Assuming: $Y = 0{\cdot}5$, $\lambda_0 = 2300$ Å, $\Delta\lambda_{\text{eff.}} = 0{\cdot}02$ Å, and $T_f = 2000°\text{K}$, the gain factor is calculated from equation 7 to be $0{\cdot}7 \times 10^8$ for $\rho^s = 3 \times 10^{-7}$ erg cm^{-3}. The integrated radiance of a Cd electrodeless discharge tube has been reported by Mansfield *et al.*[9] to be about 10^4 erg sec^{-1} cm^{-2} sterad^{-1} at 2288 Å. When this source is imaged under a solid angle of 1 sterad in the flame, the above assumed value of ρ^s could be realized. According to equation 6 this gain factor would also be attained, when under the same experimental conditions a high-pressure xenon lamp XBO 450 with radiance temperature[10] $T_s \approx 6000°\text{K}$ is used. The Osram Cd vapour lamp has been reported[10] to yield a $10\times$ higher radiance than the above Cd electrodeless lamp, so that even a gain factor exceeding 10^8 could be expected.

(c) Conclusions

It appears from the above examples, that under suitable conditions the excited state population n^* in AFS can considerably exceed the thermal value. In the calculation of detection limits for resonance fluorescence, the shot-noise of the photocurrent released by the thermal atomic emission is then irrelevant and the equations given by Jenkins[2] for the detection limit are not applicable.

The examples given also show that under suitable conditions a strong population inversion can be expected between the level excited by the source radiation, and other excitation levels that lie within, say, 1 eV distance below this level. Population inversion is known to be a necessary but not a sufficient condition for the operation of a laser.

A more specific discussion of the theoretical gain factors in AFS requires experimental data on the fluorescence yield factor Y as well as on the (spectral) radiance or radiance temperature of available light-sources. Extensive data on different types of sources have been reported by Prugger[10]. The numerical values obtained for sources that show strong spatial inhomogeneity should be carefully considered. The radiance measured by Prugger[10] for a high-pressure xenon arc, for example, appear to exceed by about one order of magnitude the values measured by Zeegers and Snelleman (personal communications). Zeegers has mapped the spatial distribution of the radiance of this source and found a strong inhomogeneity in both axial and radial directions.

There is still a great lack of experimental Y values for atomic lines belonging to elements that are of interest in practical AFS. Jenkins[2, 11–13] has reported Y values for the resonance lines of Li, Na, K, Rb, Cs and Tl; Hooymayers

and Alkemade[7], Hooymayers and Nienhuis[14] and Hooymayers and Lijnse[15] have measured Y for Na, K (4P and 5P levels) and Rb in flames with several diluent gases. Pearce, de Galan and Winefordner[16] have measured approximate fluorescence yield factors in unpremixed fuel-rich hydrogen–oxygen, acetylene–oxygen and hydrogen–argon-entrained air flames for the resonance lines of Mg, Ag, Cu, Tl, Au, Pb, Ca, Mn, Co, Fe and Cd. Turbulent mixing with the surrounding air introduces an appreciable amount of nitrogen in all three flames. Recently the low value $Y = 1{\cdot}0 \times 10^{-2}$ was found[17] for the 2852 Å Mg line in a premixed acetylene–air flame at $T = 2410°K$.

In order to promote the volatilization of elements that form stable compounds in the condensed phase, high-temperature flames are often recommended. In this respect, the fairly hot unpremixed hydrogen–oxygen flame would look promising in AFS, as the major flame constituent (water vapour) is known to have a low quenching efficiency for a number of metal lines (see ref. 5 for a survey). Since hydrogen is often reported to have a much lower quenching efficiency than oxygen (and sometimes even than water vapour), a fuel-rich hydrogen–oxygen flame may be preferred. Using the specific cross section measured by Jenkins[13] for the quenching of Tl($7^2S_{\frac{1}{2}}$) by water vapour in flames at 1400°K, one might expect that in the hydrogen–oxygen flame the fluorescence yield factor would approach its maximum value within a factor of three. Since optical transitions from the Tl($7^2S_{\frac{1}{2}}$) level occur to both the $6^2P_{\frac{1}{2}}$ ground level and the low-lying $6^2P_{\frac{3}{2}}$ excitation level, the maximum yield factor here is lower than unity when only one fluorescent line is measured[18]. These estimates of the yield factor in hydrogen–oxygen flames are rather uncertain, as turbulent mixing with the surrounding air could noticeably reduce the actual fluorescence yield[16]. The presence of a sheath of argon around the flame might be profitable in this respect.

Also the possible presence of OH radicals in significant concentrations may cause some uncertainty, as cross sections for quenching by OH are not known. However, the presence of O or H atoms can be fully neglected here, since monatomic species usually have negligible quenching efficiencies[5]. Another source of error might be the extrapolation of the experimental quenching cross section for H_2O to the higher temperature of the hydrogen–oxygen flame. Part of the quenching by H_2O is achieved by a dissociative process[5] according to

$$M^{\star} + H_2O \rightarrow M + H + OH$$

Here $M^{\star}$ and M are an excited and a ground-state metal atom, respectively. The efficiency of this dissociative quenching is expected to increase exponentially with temperature. This holds at least if the excitation energy of $M^{\star}$ (3·3 eV for the $7^2S_{\frac{1}{2}}$ Tl level) is lower than the dissociation energy of H_2O (5·2 eV). Under this condition, the dissociative quenching process is endothermic.

A comparison of the signal strengths attainable in AFS and in atomic absorption spectroscopy (AAS) under similar measuring conditions and with the same light-source has been given previously[19]. From solid-angle considerations, the maximum ratio of the signal strengths in AFS and AAS appears to be $\frac{1}{2}Y$, which is at most equal to $\frac{1}{2}$. Nevertheless, since the background noise is usually of a quite different nature with these two spectro-

scopic methods, the actual detection limit in AFS could still be better than that in AAS.

When combining the general expression for the ratio of signal strengths[19] in AFS and AAS with that for the ratio of signal strengths in AAS and FES[20] one obtains essentially the same result as that expressed by equations 6 or 7, albeit in a slightly different form. The latter equations, however, are here derived in a more direct way which does not involve Kirchhoff's law but is mainly based on kinetic considerations.

2. THE SHAPE OF THE ANALYTICAL CURVE IN ATOMIC FLUORESCENCE SPECTROSCOPY

As is well known, the experimental analytical curves in AFS show an inversion at high solution concentrations with a line source, and level off to a constant plateau with a continuum source. This holds in the usual case of resonance fluorescence involving an optical transition to or from the ground state. The shape of the curves with non-resonance fluorescence will not be considered here, but the following theoretical treatment can be easily modified to include the latter case too.

After some preliminary attempts[21,22], a more definitive theoretical treatment of the analytical curves in AFS has been given by Hooymayers[23] (see also ref. 24). In this treatment the spectral shapes of the exciting and fluorescent radiation are explicitly taken into account, which leads to rather complicated equations involving several integrations over frequency as well as spatial coordinates. As will be shown here, a more direct and simpler surveyable derivation can be given in the extreme cases of a continuum and a sharp-line source, respectively. This derivation starts from the curve-of-growth theory, which is well known in connection with the analytical curves found in FES for resonance lines.

(a) Recapitulation of the curve-of-growth theory

There is a close connection between the integral line radiance B (in erg sec^{-1} cm^{-2} $sterad^{-1}$) of a resonance emission line and the so-called integral absorption A_t of the same line seen in absorption against a continuum source. The latter quantity is defined as the integral of the wavelength-dependent absorption factor $\alpha(\lambda)$ (fraction of radiation power absorbed) over the whole line width

$$A_t \equiv \int \alpha(\lambda)\, d\lambda \tag{8}$$

When the flame temperature is homogeneous and according to Kirchhoff's law, we have in the case of thermal equilibrium

$$B = B^b_{\lambda_0} A_t \tag{9}$$

Here $B^b_{\lambda_0}$ is the spectral radiance (radiance per unit wavelength interval in Å) of a black body at flame temperature T_f and at the wavelength λ_0 of the line centre. In very good approximation $B^b_{\lambda_0}$ is given by Wien's law which contains the factor $\exp[-h\nu_0/kT_f]$. Here h and k are the Planck and Boltzmann constants, respectively, while ν_0 is the optical frequency at line centre. For resonance lines, we have $h\nu_0 = E_{exc.}$, where $E_{exc.}$ is the excitation energy.

The same exponential factor is also found in Boltzmann's law which describes the relative population $n^\star/n$ of the excited state. Thus we can also write instead of equation 9

$$B = c_1(n^\star/n)A_t \tag{10}$$

where c_1 is a constant for a given atomic line.

The factor $B^b_{\lambda_0}$ in equation 9 explains the strong, exponential dependence of the emission intensity on temperature. The factor A_t, which is but weakly dependent on temperature, describes the variation of intensity with ground-state concentration n and flame depth l. In fact, it is a function of the product nl. This function depends on the parameter a defined by $a \equiv (\ln 2)^{\frac{1}{2}}$ times the ratio of Lorentz to Doppler half-intensity width. The curve relating A_t, or some quantity proportional to it, to nl, or some other proportional quantity, is called a *curve-of-growth*. This curve describes the dependence of resonance line intensity on metal concentration in flame emission spectroscopy. *Figure 1* shows some curves for different a parameters, in a double-logarithmic plot (for calculation of the curves-of-growth, see refs. 25–27). For small concentrations all curves approach a linear asymptote ($A_t \propto nl$), whereas for high concentrations a square-root asymptote [$A_t \propto (nl)^{\frac{1}{2}}$] is attained, at least if $a \neq 0$. The deviation from the initial linear asymptote is caused by the effect of self-absorption, which is well known in flame emission analysis[28]. With regard to what follows, it is important to note from *Figure 1* that for $0 < a \lesssim 1$ the curves show an inflection. That is, the

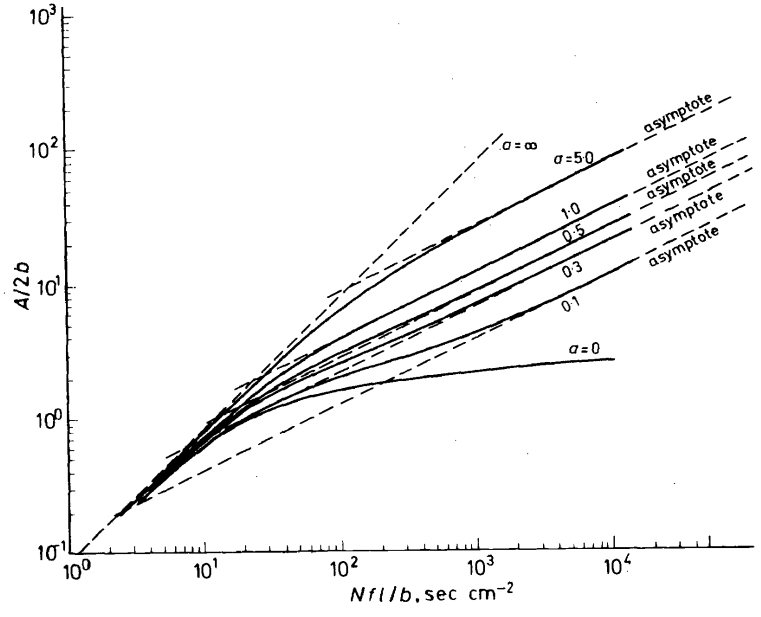

Figure 1. Theoretical curves-of-growth are shown for several a parameters ranging from 0 to 5·0. The quantity plotted on the ordinate is proportional to the 'integral absorption', while the quantity plotted on the abscissa is proportional to the atomic ground-state concentration times the flame depth. (Derived from T. Hollander, *Thesis*, Utrecht, 1964)

derivative $\gamma \equiv \mathrm{d} \log (A_t)/\mathrm{d} \log (nl)$ has a minimum value at some intermediate value of nl. This minimum value is smaller than a half, being the value attained on the asymptote for high concentrations. In contrast, for $a \gtrsim 1$ the derivative γ decreases monotonically from unity to one half for nl going from zero to infinity.

Equation 10 applies not only in equilibrium, but also when $n^\star/n$ is enhanced above its thermal equilibrium value, for example, by an exciting light-beam, as in the case of AFS. The only condition for equation 10 is that $n^\star/n$ is uniform along the line of observation. The more general validity of equation 10 may be made plausible by realizing that the dependence of the emission on $n^\star/n$ does not involve the specific way in which the excited state is populated, whether by thermal collisions or by absorption of photons. The factor A_t which describes the effect of self-absorption on the emitted radiation, is also independent of the way in which the atoms are excited. For a further discussion on the validity of equation 10 see ref. 5.

(b) General expression for the fluorescence intensity

Consider the brick-shaped flame cell shown in *Figure 2*. The concentration n of metal atoms in the ground state is assumed to be uniform. The flame is

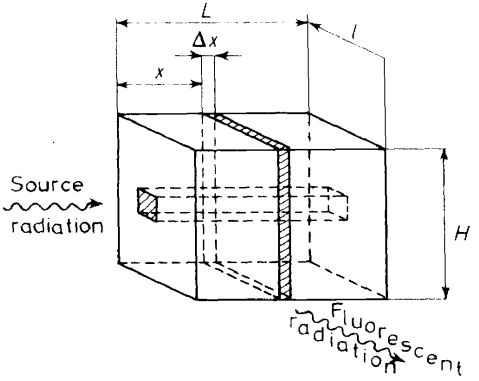

Figure 2. Dimensions of brick-shaped flame cell considered in the derivation of the analytical curve in fluorescence spectroscopy from the curve-of-growth theory

irradiated by a homogeneous beam of light perpendicular to the left-hand face. The resonance fluorescence radiation perpendicular to the front face is observed. The thermal emission of the atomic line is supposed to be eliminated by the application of a modulation technique. Thus we shall consider here only the increase $\Delta n^\star \equiv n^\star - n_{th}^\star$ in the concentration of excited atoms brought about by absorption of the primary photons. The contribution to the excitation rate from re-absorption of secondary photons is neglected. Since the exciting radiation is gradually weakened on its way through the flame along the x axis, $\Delta n^\star$ will, in general, be a function of x. Inside a thin slab of flame gas with thickness Δx (see *Figure 2*), $\Delta n^\star$ may, however, be considered to be uniform. Consequently, equation 10 can be applied to this slab to calculate the radiance $B_F(x)$ of the fluorescence line observed at distance x from the irradiated face. Thus we have

$$B_F(x) = c_1\{\Delta n^{\star}(x)/n\}A_t(nl) \tag{11}$$

$A_t(nl)$ denotes the value of A_t for a flame with atom concentration n and depth l which is measured along the line of observation. For $\Delta n^{\star}$ we have according to equation 1

$$A\,\Delta n^{\star}(x) = YU(x) \tag{12}$$

where $U(x)$ is the number of excitations per second and per cubic centimetre by photon absorption, as a function of x. Combination of equations 11 and 12 yields

$$B_F(x) = (c_1 Y/A)U(x)A_t(nl)/n \tag{13}$$

The radiant intensity ΔI_F (in erg $\sec^{-1}$ sterad^{-1}) of the fluorescence emitted by the designated flame slab with surface area $H\,\Delta x$, follows from equation 13

$$\Delta I_F = (c_1 YH/A)U(x)\{A_t(nl)/n\}\,\Delta x \tag{14}$$

The total radiant intensity I_F of the fluorescence radiation in the direction of observation, is obtained by integration over x

$$I_F = c_2\{A_t(nl)/n\}\int_0^L U(x)\,\mathrm{d}x \tag{15}$$

with: $c_2 \equiv c_1 YH/A$. The integral in equation 15 equals the number of primary photons absorbed per second in an arbitrary baulk with length L parallel to the x axis and with a cross section of 1 cm^2 (see baulk with hatched end-face in *Figure 2*). The combined dependences of this integral and of $A_t(nl)/n$ on n determine the shape of the analytical curve in AFS, at least under the idealized geometrical conditions imposed. In two extreme cases as regards the relative spectral profile of the source radiation, equation 15 leads to a simple expression, as we shall presently see.

(c) Shape of analytical curve with a continuum source

The spectral irradiance of the source radiation at the surface of the flame ($x = 0$), is denoted by E_{λ_0} (in erg $\sec^{-1}$ cm^{-2} per unit wavelength interval in Å). This quantity is assumed to be constant over the whole width of the comparatively narrow absorption line. The power absorbed in the whole baulk shown in *Figure 2* is then given by

$$\int E_{\lambda_0}\alpha(\lambda)\,\mathrm{d}\lambda = E_{\lambda_0}A_t(nL)$$

as the baulk has a length L. Thus we have

$$\int_0^L U(x)\,\mathrm{d}x = E_{\lambda_0}A_t(nL)/h\nu_0 \tag{16}$$

and with the aid of equation 15

$$I_F = c_3 A_t(nl)A_t(nL)/n \tag{17}$$

with $c_3 \equiv c_1 YHE_{\lambda_0}/Ah\nu_0$.

The close connection between the analytical curve in AFS (that is, I_F as a function of n or solution concentration) and the analytical curve in FES or the curve-of-growth (that is, A_t as a function of n) is evident. From the known shape of the latter curve for a given a parameter, the shape of the analytical curve in AFS can now be simply deduced. We note that the factor

$A_t(nL)$ in equation 17 accounts for the absorbed source radiation as a function of n, while the factor $A_t(nl)/n$ accounts for the loss of fluorescence radiation due to self-absorption. The possibility of describing these absorption effects by means of two separate factors is connected with the special geometry of the flame cell chosen.

For a given a parameter the shape of the analytical curve, plotted double-logarithmically, depends only on the *ratio* $\zeta \equiv L/l$. That is, for a given ζ-value we can always bring the analytical curve into coincidence with the curve describing $\log A_t(y)A_t(\zeta y)/y$ as a function of $\log y$ through an appropriate shift parallel to the coordinate axes.

The asymptotic behaviour of the analytical curve follows directly from equation 17, if we recall the general asymptotic behaviour of the curve-of-growth shown in *Figure 2*. When $n \to 0$, $A_t(nl)$ and $A_t(nL)$ vary as nl and nL, respectively. Thus we expect a linear asymptote $I_F \propto n^2lL/n = nlL$ for $n \to 0$.

The dependence of I_F on the oscillator strength f at the low-concentration asymptote also follows from equation 17. Curve-of-growth theory indicates that A_t will become proportional to f for $n \to 0$[6,29]. Thus we find with the help of equation 2

$$I_F \propto (Y/A)f^2 = f^2/(A + k)$$

where the transition probability A is connected to f through (see same literature)

$$fg_l = 1{\cdot}51 \times 10^{-16} \lambda_0^2 g_u A \tag{18}$$

Here g_l and g_u are the statistical weights of the lower and upper atomic levels involved in the optical transition, and λ_0 is expressed in Å. Consequently, I_F varies as f^2 as long as the yield factor Y is small compared to unity, that is, $A \ll k$. For $A \gg k$, however, I_F varies as f. Atomic resonance lines with large f values ($\simeq 1$) are thus favourable for obtaining a large signal strength in AFS. It is noted for comparison that the signal strengths obtained in AAS and FES are always proportional to f, in the limit that $n \to 0$.

For large n-values, $A_t(nl)$ and $A_t(nL)$ vary as $(nl)^{\frac{1}{2}}$ and $(nL)^{\frac{1}{2}}$, respectively, and we have

$$I_F \propto (nl)^{\frac{1}{2}}(nL)^{\frac{1}{2}}/n = (lL)^{\frac{1}{2}}$$

which is independent of n. With a continuum source, the analytical curve thus approaches a horizontal asymptote in the high-concentration range and chemical analysis is no longer possible. In the same range of high concentrations the analytical curve for FES varies as $n^{\frac{1}{2}}$ and chemical analysis is still possible here, albeit perhaps with a slightly lower precision than in the linear range. *Figure 3* (upper curve) shows a calculated analytical curve with a continuum source together with its linear and horizontal asymptotes for an assumed value $a = 0{\cdot}4$.

The appearance of a local maximum in the upper curve of *Figure 3* is to be noted. This is connected with the inflection occurring in the curve-of-growth for $a \gtrsim 1$ (see Section 2a). Because of this inflection there is an intermediate range of concentrations where the derivative γ of $\log A_t$ as a function of $\log n$ is *smaller* than the final asymptotic value $\gamma = \frac{1}{2}$. Upon differentiating $\log I_F$ with regard to $\log n$ one gets from equation 17

$$(\mathrm{d} \log I_F/\mathrm{d} \log n) = \gamma + \gamma' - 1 \tag{19}$$

where $\gamma \equiv \mathrm{d} \log A_t(nl)/\mathrm{d} \log n$, and $\gamma' \equiv \mathrm{d} \log A_t(nL)/\mathrm{d} \log n$. When for some (finite) value of n, $(\gamma + \gamma')$ just equals one, an extremum (here: a maximum)

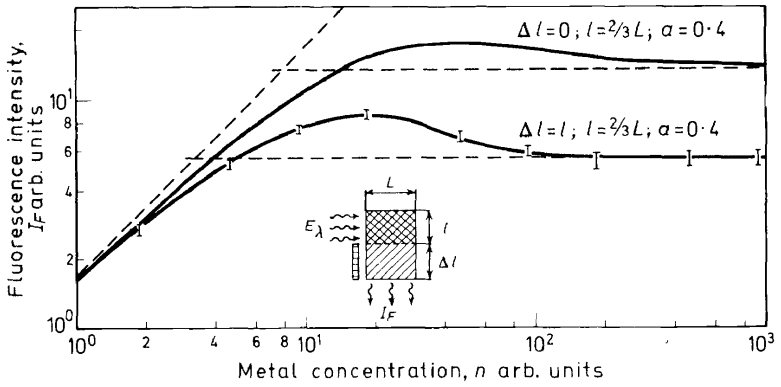

Figure 3. Fluorescence intensity I_F as a function of metal concentration n for the flame cell considered in *Figure 2*, with a continuum light-source. The upper curve was calculated for a fully illuminated flame cell, with $a = 0{\cdot}4$. The lower curve was calculated for a partially illuminated flame cell (see insert) with the same a parameter. Experimental values with their spreads are represented by vertical bars and refer to the 2852 Å Mg-line in a premixed acetylene–air flame with a xenon lamp as exciting light-source. Their relative positions are to be compared with the lower theoretical curve. (According to calculations and measurements by Zeegers)

will occur in the analytical curve. If, for example, $l = L$, this maximum is found at that value of n at which the tangent of the curve-of-growth, plotted double-logarithmically, has a slope $\tan\beta = \frac{1}{2}$. Since for $l = L$, $\gamma = \gamma' = \tan\beta$, we have here $\gamma + \gamma' = 1$.

In the limit $n \to \infty$, both γ and γ' tend to $\frac{1}{2}$ and a second extremum is attained. This extremum is identical to the constant plateau to which the curve approaches asymptotically. This (asymptotic) extremum occurs for all a values larger than zero.

The incipient deviation of the analytical curve from its initial asymptote can be found in a first order approximation as follows. According to the curve-of-growth theory, $A_t(nl)$ can be expanded[5] in a series for small values of nl

$$A_t(nl) \propto nl\{1 - \tfrac{1}{2}\overline{k(\lambda)}l + \ldots\} \tag{20}$$

with $\overline{k(\lambda)} \equiv \int k^2(\lambda)\,d\lambda / \int k(\lambda)\,d\lambda$, which is proportional to n, since $k(\lambda)$ is so. Application of this series expansion to both A_t factors in equation 17 yields

$$I_F \propto nlL\{1 - \tfrac{1}{2}\overline{k(\lambda)}(l + L) + \ldots\} \tag{21}$$

The relative deviation from linearity is thus approximately $-\frac{1}{2}\overline{k(\lambda)}(l + L)$ at sufficiently low concentrations. The corresponding relative deviation because of self-absorption in the case of FES is $-\frac{1}{2}\overline{k(\lambda)}l$ where l is the flame depth along the line of observation. When $l = L$, the concentration at which a deviation of one per cent is found, is half as small in AFS as in FES, when the same flame is used. In general, the range of linearity extends, in practice, in FES to a concentration that is $(l + L)/l$ times as high as in AFS, for a given resonance line.

When the flame cell is only *partially illuminated* by the source (as shown by the insert in *Figure 3*), the shape of the analytical curve will be affected

due to self-resersal in the non-illuminated flame layer facing the detector. It might be advantageous to illuminate only the middle portion of the flame, when turbulence at the flame border would otherwise cause the fluorescence intensity to fluctuate too strongly.

In this situation the fluorescence intensity I_F with a continuum source, can be derived directly from equation 17. Let Δl be the thickness of the non-illuminated part of the flame shown in *Figure 3* and assume that the atomic concentration is uniform throughout the flame. Obviously, I_F now equals the difference of the fluorescence intensity obtained with the flame illuminated part of the flame shown in *Figure 5* and assume that the flame part with thickness Δl illuminated. Thus we have

$$I_F = c_3 A_t(nL)\{A_t(nl + n\,\Delta l) - A_t(n\,\Delta l)\}/n \tag{22}$$

This equation is identical to that derived by Hooymayers[23] in a more complicated way involving explicitly the absorption coefficient as a function of frequency. Since all functions A_t occurring in equation 22 vary linearly with n for $n \to 0$, again a linear initial asymptote ($I_F \propto n$) is expected. The position of this asymptote is independent of Δl. When n grows large, all functions A_t behave as $n^{\frac{1}{2}}$ and I_F again approaches a horizontal asymptote. Defining $\xi \equiv \Delta l/l$, we can write equation 22 in the form

$$I_F = (c_3/n)\, A_t(nL) A_t(nl)[\![A_t\{nl(\xi + 1)\} - A_t(nl\xi)]\!]/A_t(nl) \tag{23}$$

where the left-hand principal factor (leading the square brackets) just equals the RHS of equation 17 which describes I_F for $\Delta l = 0$. The asymptotic value of I_F for $n \to \infty$ is thus found to equal the value for $\Delta l = 0$ multiplied by:

$$[\{nl(\xi + 1)\}^{\frac{1}{2}} - \{nl\xi\}^{\frac{1}{2}}]/\{nl\}^{\frac{1}{2}} = \{\xi + 1\}^{\frac{1}{2}} - \xi^{\frac{1}{2}}.$$

The lower curve drawn in *Figure 3* was calculated for $\xi = 1$. The initial asymptote is, indeed, seen to coincide with that of the upper curve ($\Delta l = 0$), whereas the height of the horizontal asymptote is $(\sqrt{2} - 1) = 0{\cdot}41$ times that of the upper curve.

The right-hand principal factor in equation 23 is unity for $n = 0$ and approaches a value $\{(\xi + 1)^{\frac{1}{2}} - \xi^{\frac{1}{2}}\}$, being smaller than unity, for $n \to \infty$. In the intermediate range of concentrations where the curve-of-growth $A_t(nl)$ changes over from a linear to a square-root dependence, the decrease of this factor with increasing concentration is most pronounced. Because of this additional decreasing factor, the local maximum in the lower curve of *Figure 3* ($\xi = 1$) is more accentuated than that in the upper curve ($\xi = 0$) where this factor is unity.

In the special case $\xi = 1$, the curve relating $\{A_t(2nl) - A_t(nl)\}/A_t(nl)$ to nl is called the duplication curve. It describes the relative increment in flame emission as a function of n when a mirror is placed behind the flame[27]. The detailed course of this curve depends on the a parameter and has been discussed in the literature cited.

Since the final value $\{(\xi + 1)^{\frac{1}{2}} - \xi^{\frac{1}{2}}\}$ of the right-hand principal factor in equation 23 drops to zero for large ξ, the rate of decrease of this factor with increasing n and thus the appearance of the local maximum will become the more pronounced, the larger is ξ. The presence of a non-illuminated absorbing layer in the flame may give rise to a local maximum even when $a > 1$ where the curve for $\Delta l = 0$ shows no maximum at all (see above).

This is clearly demonstrated in the curve for $a = 5{\cdot}0$ in *Figure 2* of Hooymayers[23], calculated for the case $\Delta l/l = 1{\cdot}5$.

These theoretical calculations have recently been confirmed experimentally by Zeegers (to be published) at the Department of Chemistry in the University of Florida at Gainesville. The vertical bars in *Figure 3* show the experimental values with their spreads for the 2852 Å Mg line in a rectangular, premixed acetylene–air flame with $l = \frac{2}{3}L$ and $a = 0{\cdot}4$. The flame was partially illuminated by a xenon lamp. The a parameter was determined independently. The agreement with the calculated (lower) curve is excellent. The measurements are shown in *Figure 3* in arbitrary units, but were actually done on an absolute scale. The absolute intensity values appeared to be consistent with the value $1{\cdot}0 \times 10^{-2}$ for the fluorescence yield factor Y determined independently.

The spectral shape of the fluorescent line is not explicitly considered in this treatment. For the model considered here, the relative spectral shape of the fluorescent resonance line is the same as that of the thermally excited line, for equal values of atom concentration and flame depth. In both cases, the line appears to be broadened by self-absorption to the same extent. For $\Delta l > 0$, an additional self-reversal effect exists. The latter effect would also be expected for a thermally excited line that is observed through a cool outer layer with the same thickness Δl and metal concentration. In this comparison the weak dependence of A_t on the actual temperature in the outer layer is disregarded.

When the fluorescence is observed over only a part of the illuminated flame cell (see insert of *Figure 4* when we take $\Delta l = 0$), the intensity as a function of n can again be described by equation 23 if we interchange l and L therein. This holds because of the symmetrical way in which l and L occur in equation 17 from which equation 23 was derived. The analytical curves found in this case are similar to that shown in *Figure 3*, and the same discussion applies as before. The only difference from the former case is that the relative spectral shape of the fluorescence line is not affected.

(d) Shape of the analytical curve with a narrow-line source

We now consider the other extreme case, namely when the spectral linewidth of the source is small compared to that of the absorption line. The integral irradiance of the source line at the surface of the flame is denoted by E (in erg $\sec^{-1}$ cm^{-2}). The fraction of source radiation absorbed per centimetre path length is assumed to be practically equal to the peak absorption coefficient k_m. According to Beer's law the number of primary photons absorbed per second in the baulk considered in *Figure 2* is

$$\int_0^L U(x)\,\mathrm{d}x = (E/h\nu_0)\,(1 - \exp\,[-k_m L])$$

For I_F we then get from equation 15

$$I_F = c_4 A_t (nl)\,(1 - \exp\,[-k_m L])/n \qquad (24)$$

with $c_4 \equiv c_2 E/h\nu_0$.

Considering the asymptotic behaviour of A_t and expanding the exponential function in a series, we find for small n-values approximately

$$I_F \propto nlk_m L/n = k_m lL$$

where k_m is proportional to n. Thus again an initial linear asymptote ($I_F \propto n$) exists. In contrast to the continuum case, the slope of this asymptote now depends on k_m and thus on the spectral width of the absorption line.

For high concentrations the exponential function drops to zero, that is, practically all the primary photons become absorbed while $A_t(nl)$ behaves as $(nl)^{\frac{1}{2}}$ (for $a > 0$). We then get from equation 24: $I_F \propto 1/n^{\frac{1}{2}}$. The position of the high-concentration branch (with negative slope) of the analytical curve is insensitive to changes in L, but still depends on l.

Since the curve rises at low concentrations and decays to zero for high concentrations, a maximum will occur for all values of the a parameter. This maximum is positioned at some intermediate n value, where simultaneously the fluorescence intensity becomes markedly affected by self-absorption and k_mL is no longer small compared to unity. In a double-logarithmic plot the analytical curve has thus an initial asymptote with positive slope $\tan\beta = 1$, and a final asymptote with negative slope $\tan\beta = -\frac{1}{2}$. The shape of the curve and the point of intersection of these asymptotes depend on the a parameter (see the curves calculated by Hooymayers[23]).

The incipient deviation from the initial asymptote ($I_F \propto n$) in the low-concentration range can be calculated as follows. Expanding $\exp[-k_mL]$ as well as $A_t(nl)$ in a series (see equation 20) we get from equation 24 in second order of n

$$\begin{aligned} I_F &\propto \{1 - \tfrac{1}{2}\overline{k(\lambda)}l\}(1 - \tfrac{1}{2}k_mL)k_mL \\ &\approx k_mL\{1 - \tfrac{1}{2}\overline{k(\lambda)}l - \tfrac{1}{2}k_mL\} \end{aligned} \tag{25}$$

Here k_m and $\overline{k(\lambda)}$ are both proportional to n. The relative deviation from the initial asymptote for small values of n is thus $-\frac{1}{2}\overline{k(\lambda)}\{l + Lk_m/\overline{k(\lambda)}\}$. Comparing this with the corresponding equation 21 for a continuum source, we see that under similar flame conditions the analytical curve with a line source begins to deviate from a linear relationship at a lower concentration. This holds because $k_m/\overline{k(\lambda)}$ is always larger than unity. The latter ratio depends on the relative spectral shape of the absorption coefficient $k(\lambda)$, that is, on the a parameter. In ordinary flames at 1 atm this ratio is about 1·4 for the yellow Na doublet. There will be no great difference, then, between a line and a continuum source as regards the concentration range in which the analytical curve is practically linear.

When only part of the observed flame cell is illuminated or (and) the fluorescence from only a part of the illuminated cell is observed (see insert in *Figure 4*), the shape of the analytical curve will again be affected. The presence of a non-illuminated absorbing layer with thickness Δl causes a self-reversal effect which can be calculated in complete analogy with the continuum case. As a result, we find that the high-concentration branch is displaced downward by a constant factor. The slope of the asymptote for $n \to \infty$ in a double-logarithmic plot thus remains the same. Analytical curves for a flame with a rectangular cross section and with $\Delta l/l = 1{\cdot}5$ have been calculated by Hooymayers[23] for various a parameters.

The partial absorption of the source radiation in a layer with thickness ΔL between the source and the observed part of the flame affects the analytical curve more markedly. For a narrow-line source the fraction of radiation

transmitted by this layer equals $\exp[-k_m \Delta L]$ according to Beer's law. We find I_F as a function of n by multiplying c_4 in equation 24 by this fraction

$$I_F = c_4 A_t(nl) \exp[-k_m \Delta L](1 - \exp[-k_m L])/n \qquad (26)$$

For high concentrations, that is for $k_m L \gg 1$ and $A_t(nl) \propto n^{\frac{1}{2}}$, I_F varies with n practically as $\exp[-k_m \Delta L]/n^{\frac{1}{2}} \equiv \exp[-c_5 n]/n^{\frac{1}{2}}$, with $c_5 \equiv k_m \Delta L/n$. Through this additional exponential factor the fluorescence intensity becomes strongly depressed when n grows large. The relative decrease of I_F per unit concentration interval, that is $-(\mathrm{d}I_F/\mathrm{d}n)/I_F$, is the stronger, the larger is ΔL. In other words, this *relative* decline of I_F at the high-concentration branch can be made arbitrarily strong, by choosing ΔL sufficiently large. However, when we relate the analytical sensitivity to the variation in concentration for which I_F decreases by one per cent, AFS provides no substantial advantage over AAS when applied to a similar flame with absorption path length ΔL. We note that the *absolute* decline, $-\mathrm{d}F/\mathrm{d}n$, at the high-concentration branch becomes just the smaller, the larger is ΔL. From the point of view of absolute signal strengths, this branch is not suitable for the measurement of small variations in n.

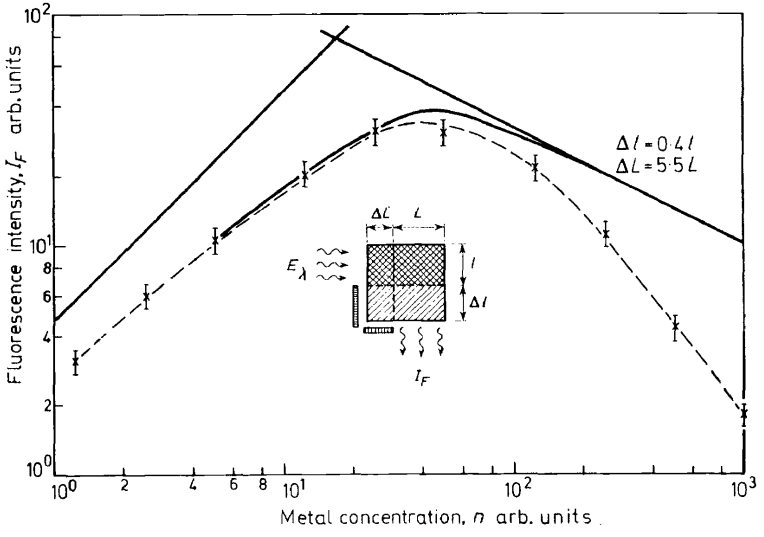

Figure 4. Fluorescence intensity I_F as a function of metal concentration n in the case of a partially illuminated flame cell (see insert) and for a narrow-line source. The full curve with its initial and final asymptotes is calculated for $\Delta L = 0$, $l = 5L$, $\Delta l = 0{\cdot}4l$ and $a = 0{\cdot}4$. The broken curve was measured for the 2852 Å Mg-line in a premixed acetylene air flame with $\Delta L = 5{\cdot}5L$, $l = 5L$, and $\Delta l = 0{\cdot}4l$, with a microwave discharge Mg-lamp as primary light-source. Comparison of the full curve with the broken curve shows the effect of partial observation of the illuminated flame cell ($\Delta L \neq 0$). (According to calculations and measurements by P. J. Th. Zeegers.)

This particular effect of an absorbing layer with thickness ΔL between the light-source and the observed flame section has been experimentally checked by Zeegers[17]. The analytical curve was measured on an absolute scale with a microwave discharge lamp emitting the 2852 Å Mg line, under similar condi-

tions as prevailing in the measurements shown in *Figure 3* for a continuum source. The relevant path lengths and flame dimensions are shown in *Figure 4*, where the analytical curve is plotted in arbitrary units for two values of ΔL. The value of L is not very relevant as far as the high-concentration branch is concerned (see above). The curves in the double-logarithmic plot were shifted so that their initial and final asymptotes, which would be approached when ΔL equalled zero, coincided. The position of the final asymptote for $\Delta L = 0$ was calculated from additional measurements of the a parameter, Δl etc. The experimental curves for $\Delta L \neq 0$ clearly deviate from the latter asymptote the more so, the larger are n and ΔL. These deviations appear to be reasonably well described by an exponential factor, conforming to theory (see above).

(e) Conclusions

It should be well borne in mind that the quantitative relations in this Section are derived under rather idealized conditions. In practical situations deviations from the calculated shape of the analytical curve can be expected because these conditions may not be fulfilled.

(i) The atomic source line may not usually be considered as extremely sharp compared to the absorption line-width. A correction may be made for this deviation by replacing k_m in equation 24 by an effective value $\bar{k}$ which is smaller. An approximate expression for $\bar{k}$ has been given[30] in terms of the a parameter and the ratio of half-widths of the source and absorption line. It should be realized, however, that the relative spectral distribution of the exciting radiation continuously varies on its way through the flame at strong absorptions. Since the centre of the exciting line is more strongly absorbed than the line wings, an apparent broadening and even a self-reversal of the exciting line may occur inside the flame. This effect will not be very significant when at high concentrations practically all incoming source radiation is absorbed within the observed flame section ($\Delta L = 0$; see insert in *Figure 4*). However, when $\Delta L \neq 0$ and $k_m \Delta L \gg 1$, the intensity of the source radiation incident on the actually observed flame section may not be accurately described by Beer's law with an effective absorption coefficient that is *in*dependent of n. It is noted that even a small difference Δk in absorption coefficient will result in a large difference in transmitted radiation power, when at high concentrations $(\Delta k)^{-1}$ becomes less than the absorption path length. When, for example, for a certain wavelength (λ), k deviates by ten per cent from the peak absorption coefficient at λ_0, a difference of a factor three in transmitted power at λ and λ_0, respectively, may be expected with the yellow Na-line in a premixed flame with thickness of 1 cm, fed by spraying a 1000 p.p.m. sodium solution.

(ii) The geometry of the whole flame as well as of its illuminated and observed sections is usually different from that assumed in the theoretical analysis. In particular, the detailed shape of the curves with a cylindrical flame will deviate markedly from the curves shown in *Figures 3* and *4*. For the latter kind of flame the exact theoretical expressions are much more complicated.

(iii) Due to spatial inhomogeneity of the lamp radiance, the density of the exciting radiation may not be uniform over the illuminated flame surface.

The relative excited state population n^*/n is then not uniform inside the thin flame slab with thickness Δx considered in *Figure 2*. Thus no simple expression can be given for the fluorescent radiance of this flame slab at arbitrary concentrations. Similar difficulties may arise with turbulent flames where the fluorescence yield factor Y could vary with distance from the axis because of the entrainment of nitrogen from the surrounding air.

(iv) The given expressions for I_F are not strictly applicable when the solid angle under which the source radiation enters the flame is large. Light rays traversing the flame under different directions will not undergo the same absorption. A similar conclusion holds for the degree of self-absorption of the fluorescence radiation, when light rays with largely different directions are collected by the optical measuring system. This complication also arises when a thermally excited resonance line is observed in FES under a large solid angle. However, if the maximum angle between different light rays is less than 30°, the deviation from the given formulae is still unimportant[23].

All these considerations together may easily explain why the shape of the curves observed in practical flame analysis does not accurately conform to the theoretical equations. It is to be recalled that the experimental values plotted in *Figures 3* and *4* were obtained under special experimental conditions which closely agreed with those assumed in the theory. Under the usual practical conditions the local bump expected from theory for a continuum source might be smeared out and not appear at all. Some practical curves showed a sublinear behaviour over a surprisingly long range of low concentrations with a continuum source[31]. An explanation has not yet been offered.

The theoretical discussion presented may still have some value with regard to practical curves. It provides a general physical understanding of the appearance of a plateau in the case of a continuum source, and of a maximum in the case of a line source. These features have been observed frequently in analytical applications of AFS. The theoretical calculations may also give a general insight into the influence of the flame dimensions in the direction of the source and of the spectrometer upon the deviation from the initial linear asymptote. This influence appears to be not very different for a continuum and a line source. The discussed effects on the analytical curve of partial illumination or partial observation of the illuminated flame cell may be instructive in practical applications too.

The plateau in the analytical curve with a continuum source is, of course, of no practical use. The discussion on the declining branch of the curve with a line source at high concentrations might be of some interest when the applicability of this branch for practical analysis is questioned.

Apart from the point of view of analytical applications, the shape and absolute position of the analytical curve is also of interest in theoretical flame studies because of its relation to the a-parameter and the fluorescence yield factor[17, 23].

3. THE YIELD OF NON-RESONANCE FLUORESCENCE

(a) Introduction

When the exciting line and the observed fluorescence line are different, we speak of *non-resonance fluorescence* (see for a general introduction refs.

21, 29, 32). Some examples of non-resonance fluorescence are shown schematically in *Figure 5* for an atom with two excitation levels (1 and 2) and a ground level (0). In the case of *Figure 5*(a) and (b) different optical transitions to and from the same upper level (2) are involved (*direct line fluorescence*). In the case of *Figure 5*(c) and (d) the upper levels of the exciting and the

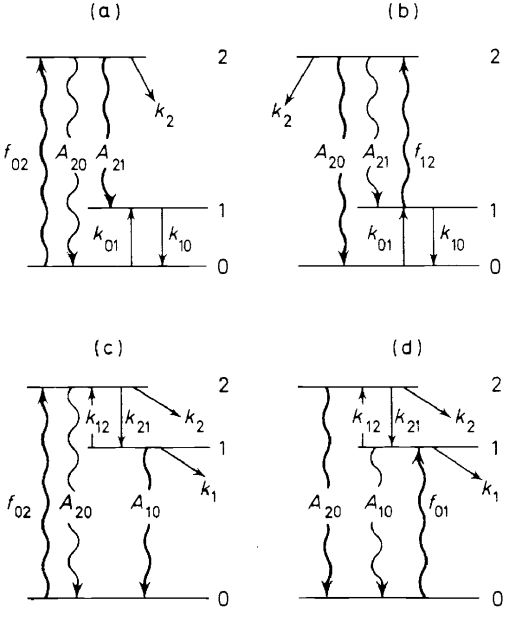

Figure 5. Three-level model of atom showing non-resonance fluorescence (direct line fluorescence in case a and b; stepwise line fluorescence in case c and d). The optical transition involved in the photo-excitation process is denoted by a bold arrow pointing upwards. The optical transition involved in the observed fluorescence radiation is indicated by a bold arrow pointing downwards. Concurrent optical and collisional transitions are indicated by thin wavy and straight arrows, respectively

fluorescence line are different (*stepwise line fluorescence*). Atoms excited to one of the upper levels are transferred to the other excitation level from which the fluorescence is observed. This transfer is usually achieved by a radiationless transition induced by collisions with flame molecules. In cases b and d the frequency of the fluorescence line is greater than that of the exciting line (so-called anti-Stokes fluorescence). The deficit in photon energy is supplied by the thermal energy of the collision partners. We are dealing here with an example of thermally assisted fluorescence[33]. In the reverse cases a and c the excess photon energy is usually converted into thermal energy.

An example of cases a and b is thallium which has a low-lying excitation level ($6^2P_{\frac{3}{2}}$) at 0·97 eV above the $6^2P_{\frac{1}{2}}$ ground level, and a higher excitation

level ($7^2S_{\frac{1}{2}}$). Optical transitions can occur between the latter excitation level and the ground level at 3775 Å, and between the two excitation levels at 5350 Å. The strength of the non-resonance absorption line at 5350 Å depends on the population of the $6^2P_{\frac{3}{2}}$ state, which is but a small fraction (about 0·02) of the ground-state population at $T = 2400°K$.

Examples of cases c and d are the alkali atoms having doublet levels ($^2P_{\frac{1}{2}}$ and $^2P_{\frac{3}{2}}$) which are optically connected to the $^2S_{\frac{1}{2}}$ ground level. The energy separation of these doublet levels increases in the order: Na–K–Rb–Cs from 0·002 to 0·07 eV. The separation of the first resonance doublet of lithium is too small to be of practical interest in flames.

In practical spectroscopic applications non-resonance fluorescence may have some advantages over resonance fluorescence. Scattering problems can be avoided by removing the spectral line used for excitation from the fluorescence spectrum. Further, the spectral line used for excitation may lie in a wavelength interval where the flame emits a strong (fluctuating) background. It could then be advantageous to measure the fluorescence at a different line outside this interval[2]. In some cases, non-resonance fluorescence yields a higher photon flux than resonance fluorescence. For example, when Tl atoms are excited at 3775 Å, the flux of photons re-emitted at 5350 Å is twice as large as the flux re-emitted at the same resonance line[18]. Since photo-(multiplier) tubes are essentially quantum detectors, it is appropriate to compare here the *photon* flux, and not the radiation *power*.

Finally, it may also be profitable to use a fluorescent line that does not terminate at the ground level, in order to avoid self-absorption losses at higher concentrations. This has, moreover, the advantage that the analytical curve with a continuum source does not level off to a constant plateau. This would otherwise make analytical determinations impossible at high concentrations. When the fluorescent line is not a resonance line, the factor $A_t(nl)/n$ in equation 17 is practically independent of n. The dependence of I_F on n is then determined by the factor $A_t(nL)$ only. In this case, the shape of the analytical curve is identical to that when the line used for excitation is observed in FES, for equal flame depth L.

In this Section we shall compare theoretically the photon yields in the case of non-resonance fluorescence that are to be expected when one line or the other is used for excitation, respectively. In Section 3b we shall derive from general theoretical relationships the conditions under which case a or case b in *Figure 5* can yield the larger photon flux. In Section 3c a similar discussion will be given for cases c and d. Practical problems in the application of non-resonance fluorescence are not dealt with. The general conclusions drawn are illustrated by arbitrary examples which may themselves be of little practical interest. However, they are believed to be helpful as a first guide in any systematic search for optimum measuring conditions.

For simplicity's sake we restrict ourselves to the linear branch of the analytical curve, that is, to the range of small concentrations n. Consequently self-absorption of the fluorescent radiation will be disregarded and the fraction of primary radiation absorbed is assumed to be proportional to n. The metal concentration, temperature and radiation density in the flame are, moreover, assumed to be homogeneous.

(b) Direct-line fluorescence

See *Figures* 5(a) and (b). Quantities relating to transitions between any pair of atomic levels are indicated by the corresponding level numbers (0, 1 or 2) as suffix. Similarly we have n_0, n_1 and n_2 for the concentrations of atoms in the corresponding states shown in *Figure 5*. The central wavelength and frequency of the optical transition between levels 0 and 1 are denoted by λ_{01} and ν_{01}, the oscillator strength for the corresponding absorption line is f_{01}, while the Einstein transition probability for the same line in emission is A_{10}.

Consider first case a where excitation occurs at λ_{02} only and fluorescence is observed at λ_{12} ($\lambda_{12} > \lambda_{02}$). Let the flame be uniformly illuminated by a *continuum source* (through an appropriate filter) with a spectral irradiance $E_{\lambda_{02}}$ (erg $\sec^{-1}$ cm^{-2} per unit of wavelength interval in Å). When a narrow-line source is used, we simply have to replace $E_{\lambda_{02}}$ everywhere by $E_{02}/\Delta\lambda_{02}$. Here E_{02} is the integral irradiance of the exciting line (in erg $\sec^{-1}$ cm^{-2}) and $\Delta\lambda_{02}$ is the effective spectral width (in Å) of the absorption line at λ_{02} in the flame (see also Section 1b).

The number F_{21} of secondary photons emitted per second at λ_{12} equals the number of photons absorbed per second at λ_{02} multiplied by the yield factor (also called quantum efficiency) of the fluorescence process considered. This yield factor is $A_{21}/(A_{20} + A_{21} + k_2)$ where k_2 is the total quenching rate constant per second for state 2 due to radiationless transitions to other states. Using a well-known expression for the integrated absorption coefficient[6, 29], we find for F_{21} (case a)

$$F_{21} = CE_{\lambda_{02}} f_{02} \lambda_{02}^3 n_0 A_{21}/(A_{20} + A_{21} + k_2) \tag{27}$$

where the constant C depends on the geometry of the illuminated flame cell but not on the atomic parameters.

In the opposite case b, we have by analogy for the number F_{20} of secondary photons emitted per second at λ_{02}

$$F_{20} = CE_{\lambda_{12}} f_{12} \lambda_{12}^3 n_1 A_{20}/(A_{20} + A_{21} + k_2) \tag{28}$$

From equations 27 and 28 we get

$$\frac{F_{20}}{F_{21}} = \frac{E_{\lambda_{12}}}{E_{\lambda_{02}}} \frac{f_{12} A_{20}}{f_{02} A_{21}} \left(\frac{\lambda_{12}}{\lambda_{02}}\right)^3 \frac{n_1}{n_0} \tag{29}$$

Assuming that the relative population of level 1 (with excitation energy E_1 and statistical weight g_1) conforms to Boltzmann's law at flame temperature T_f, we have for n_1/n_0

$$n_1/n_0 = (g_1/g_0) \exp\left[-E_1/kT_f\right] = (g_1/g_0) 10^{-5040 V_1/T_f} \tag{30}$$

Here V_1 is the excitation potential expressed in volts. Because of the fundamental relationship between f and A (equation 18) we have

$$(f_{12}/A_{21})(A_{20}/f_{02}) = (\lambda_{12}/\lambda_{02})^2 (g_0/g_1) \tag{31}$$

Substituting equations 30 and 31 into equation 29 we get

$$\frac{F_{20}}{F_{21}} = \frac{E_{\lambda_{12}}}{E_{\lambda_{02}}} \left(\frac{\lambda_{12}}{\lambda_{02}}\right)^5 \cdot 10^{-5040 V_1/T_f} \tag{32}$$

This equation clearly shows the strong dependence on V_1/T_f of the fluorescence signal in case b when compared to case a. For $T_f = 2500°K$ and $V_1 = 1$ V the exponential factor is about 10^{-2}. This bad effect may be (partly) compensated for by a large value of the pre-exponential factors occurring in equation 32, as we shall presently investigate. It is curious to note that the ratio F_{20}/F_{21} is independent of the A and f values as well as of the quenching rate constant and statistical weight factors of the levels involved.

Consider first the case when a continuum source is used for excitation, and let the ratio $E_{\lambda_{12}}/E_{\lambda_{02}}$ be identical to that for an (imaginary) black body with temperature T_c. We may formally consider T_c as the 'colour temperature' of the source. Using Wien's law for black-body radiation:

$$E_\lambda^b \propto \lambda^{-5} \exp[-h\nu/kT]$$

we can formally express $E_{\lambda_{12}}/E_{\lambda_{02}}$ in T_c. Thus we get, while replacing $(h\nu_{02} - h\nu_{12})$ by E_1,

$$F_{20}/F_{21} = 10^{5040V_1(T_c^{-1} - T_f^{-1})} \tag{33}$$

This simple expression retains only V_1 as atomic parameter, while the source and flame are solely characterized by T_c and T_f, respectively. We conclude from the latter equation that case b becomes even more favourable than case a when $T_c < T_f$. The bad effect of a relatively low population of state 1 is then overcompensated by a large ratio of $E_\lambda\lambda^5$ at the two wavelengths compared. When $V_1 = 1$ V, $T_c = 5000°K$ and $T_f = 2500°K$, the fluorescence photon flux is lower by a factor of only ten in case b than in case a, although $n_1/n_0 = 2 \times 10^{-2}$ according to Boltzmann's law.

For a tungsten strip lamp T_c is estimated to be about 3000°K in the visible and near-ultra-violet part of the spectrum, whereas T_c may even exceed 5000°K for the high-pressure xenon arc (compare Prugger[10]). It is noted that the 'colour temperature' T_c may differ from the radiance temperature T_s defined in Section 1a. However, for a black body both temperature values are identical to the true temperature of the radiating body. In general T_c may depend on the wavelengths of the atomic lines compared.

When an *atomic line source* is used for irradiating the flame at either λ_{02} or λ_{12}, we have to replace the spectral irradiance E_λ in equation 32 by $E/\Delta\lambda$, as mentioned above. If we disregard self-absorption in the atomic light-source and optical losses, the total intensities of the exciting lines at λ_{02} and λ_{12} are in the proportion: $A_{20}h\nu_{02}:A_{21}h\nu_{12}$, since the lines originate from the same upper level 2. Assuming that the effective width $\Delta\lambda$ of the absorption line in the flame is determined mainly by Doppler broadening, we have $\Delta\lambda_{02}/\Delta\lambda_{12} = \lambda_{02}/\lambda_{12}$. Consequently equation 32 reads, for a narrow-line source,

$$\frac{F_{20}}{F_{21}} = \frac{A_{21}}{A_{20}}\left(\frac{\lambda_{12}}{\lambda_{02}}\right)^3 10^{-5040V_1/T_f} \tag{34}$$

For the case of thallium with $V_1 \approx 1$ V mentioned in Section 3a and with $T_f = 2500°K$, we find from this equation

$$\frac{F_{3775}}{F_{5350}} = \frac{1{\cdot}0 \times 10^8}{5 \times 10^7} \left(\frac{5350}{3775}\right)^3 10^{-2} = 5{\cdot}5 \times 10^{-2}$$

When the non-resonance Tl-line at 5350 Å is chosen for excitation, the fluorescence photon flux measured at 3775 Å is thus about 20 times as small as in the reverse case. However, self-absorption or even self-reversal of the resonance line at 3775 Å in the source could appreciably reduce this factor.

In the case of direct-line fluorescence, we conclude that the reduction in fluorescence signal when the non-resonance line is used for excitation, need not be as bad as expected from the Boltzmann occupation of the lower level. Even when the lower level of the non-resonance line lies 1 eV above the ground level, this reduction may not be insurmountable in practice for flame temperatures above 2000°K. It depends on other, circumstantial factors whether this loss in fluorescence signal is compensated by a lower background noise, etc.

When atoms are raised from state 1 to state 2 by absorption of a strong radiation beam, a depletion of the lower excitation level 1 could result. This reduction of n_1 would unfavourably affect the fluorescence signal according to equation 28. The magnitude of this depletion can be roughly estimated by kinetic considerations. It can be shown that under practical conditions the deviation of the actual value of n_1 from the thermal equilibrium value $(n_1)_e$ might be at most of the order of one per cent.

Let the number of optical transitions from state 1 to state 2 per second and per cubic centimetre, induced by the source radiation, be given by $k'_{12}n_1$. The balance equation for the stationary population n_1 then reads

$$n_1(k_{10} + k'_{12}) = n_0 k_{01} \tag{35}$$

where k_{10} and k_{01} are the rate constants of collisional (de-)excitation of level 1 [*Figure* 5(b)]. Other radiative or radiationless transitions to or from this level are considered unimportant. In thermal equilibrium (that is, without external field) we have the balance equation

$$(n_1)_e k_{10} = (n_0)_e k_{01} \tag{36}$$

Making the quite plausible approximation $n_0 = (n_0)_e$, we find by combination of equations 35 and 36

$$n_1/(n_1)_e = k_{10}/(k_{10} + k'_{12}) \tag{37}$$

The relative deviation of n_1 from $(n_1)_e$ will be less than one per cent if k'_{12}/k_{10} is less than 10^{-2}. For excitation levels lying at least some tenths of an electron volt above the ground level the quenching rate constant k_{10} is expected to range roughly from 10^7 to 10^9 sec^{-1} in flames at 1 atm. The precise value depends among other things on whether argon or nitrogen is used as diluting gas[5]. We note that k_{10} is not expected to depend critically on the excitation energy E_1 or flame temperature.

An upper estimate of k'_{12} at 6200 Å can be made when the intense high-pressure xenon lamp calibrated by Prugger[10] is used as exciting source. A spectral irradiance $E_\lambda \approx 10^6$ erg sec^{-1} cm^{-2} per unit wavelength interval in Å may be attained if this source is imaged under a solid angle of one sterad on the flame. Making use of the theoretical expression for the integrated absorption coefficient[29], we get

$$k'_{12} = 10^{-20} \times (E_\lambda/h\nu_{12})\lambda_{12}^2 f_{12} = 1{\cdot}2 \times 10^5 f_{12}\ \text{sec}^{-1} \tag{38}$$

where λ_{12} is expressed in Å and $h\nu_{12}$ in ergs. Even when f_{12} is unity, k'_{12} will still be at least 100 times smaller than the quenching rate constant k_{10}. We may thus safely neglect the depletion of

the lower level by photon absorption. This qualitative conclusion is expected to be true for other wavelengths too.

(c) Stepwise line fluorescence

See *Figures 5*(c) and (d). Since here the photo-excited state and the state from which the observed fluorescence is emitted are different, efficient coupling between these states is a pre-requisite for the appearance of useful fluorescence. We assume here that this coupling or mixing is achieved by collisions. In the case of *Figure 5*(c) this implies that the collisional rate constant k_{21} should at least be comparable to the sum of A_{20} and the quenching rate constant k_2. The major constituent of the flame gas should thus have a small quenching cross section, as well as a relatively large mixing cross section for the states concerned. This condition is not fulfilled for the alkali doublet levels in flames burning with air, as nitrogen is an efficient quencher. For rubidium and caesium the quenching cross section of nitrogen is even larger than its mixing cross section. In flames diluted by a noble gas efficient mixing and low quenching of the Na- and K-doublet levels can be expected. The mixing rates for the Rb- and Cs-doublets having larger energy separations might be too small in these flames to compete with the radiative de-excitation rates. A general survey of recent data and interpretations has been given by Alkemade and Zeegers[5].

When mixing becomes fast enough compared to all other radiative or radiationless transitions, a partial equilibrium will be maintained between the populations of both excitation levels. The *ratio* of their populations is then practically the same as in thermal equilibrium and obeys Boltzmann's law

$$n_2/n_1 = (g_2/g_1) \exp\left[-(E_2 - E_1)/kT_f\right]$$

The rate of transitions $1 \rightarrow 2$ then balances the rate of the reverse transitions $2 \rightarrow 1$. This holds irrespective of whether level 1 or level 2 is primarily excited by the source, or whether the quenching rates k_1 and k_2 are equal or not.

If this partial equilibrium applies, a simple expression can be derived for the ratio F_{20}/F_{10} of fluorescence signals obtained in case d and c of *Figure 5*, respectively. Suppose first that a *continuum source* is used to excite directly atoms from the ground state to either state 1 or state 2. The ratio F_{20}/F_{10} is determined by the corresponding ratio of photo-excitation rates, the ratio of optical transition probabilities A_{20}/A_{10}, and the constant proportion in which the excited atoms are distributed over the levels 2 and 1. We thus find by similar calculations as given in Section 3b, while taking $\lambda_{01} \approx \lambda_{02}$ here,

$$\frac{F_{20}}{F_{10}} \approx \frac{E_{\lambda_{01}}}{E_{\lambda_{02}}} \frac{f_{01}A_{20}g_2}{f_{02}A_{10}g_1} \exp\left[-(E_2 - E_1)/kT_f\right] \tag{39}$$

Making use of equation 18, we have $f_{01}A_{20}/f_{02}A_{10} = g_1/g_2$, so that

$$\frac{F_{20}}{F_{10}} \approx \frac{E_{\lambda_{01}}}{E_{\lambda_{02}}} 10^{-5040\,\Delta V/T_f} \tag{40}$$

where ΔV is the difference in excitation potentials (in volts) of the two excitation levels. We note that the ratio F_{20}/F_{10} does not explicitly contain the oscillator strengths, optical transition probabilities or statistical weights (compare equation 32).

When we formally describe $E_{\lambda_{01}}/E_{\lambda_{02}}$ by a colour temperature T_c, as in Section 3b, we can write instead of equation 40

$$\frac{F_{20}}{F_{10}} = 10^{5040\,\Delta V(T_c^{-1} - T_f^{-1})} \tag{41}$$

which is analogous to equation 33. For $T_c \simeq T_f$, the fluorescence signal is the same in case d as in case c, irrespective of ΔV. For $T_c > T_f$, case c gives the larger signal. However, since ΔV is smaller than 0·1 V for the first resonance doublets of the alkali atoms, the difference in fluorescence signals is small in this case.

When a *narrow-line source* is used for excitation, we have to replace $E_{\lambda_{01}}/E_{\lambda_{02}}$ in equation 40 by the corresponding ratio of integrated line intensities, if the effective widths of the two absorption lines are equal. The latter assumption is reasonable for the components of the alkali doublets in flames. In the case of the Na *D*-doublet where the exponential factor in equation 40 is virtually unity, the fluorescence signals are in the proportion of the exciting line intensities. If no self-absorption occurs in the light-source, the ratio of line intensities equals the ratio of statistical weights. Thus we have for sodium $F_{20}/F_{10} = g_1/g_2 = \frac{1}{2}$. The fluorescence signal is then twice as large in case c as in case d. However, when strong self-absorption occurs in the light-source, the peak intensities of the exciting doublet lines may become nearly equal, and about the same fluorescence signal may be expected in the two cases. The peak intensities, and not the total line intensities are relevant here, because at strong self-absorption the width of the source lines may markedly exceed the absorption line widths at low metal concentrations in the flame.

The equations derived in this Section are valid under rather special conditions only. The conditions of strong collisional mixing of the two excitation levels might not easily be met when their energy separation exceeds, say, 0·01 eV. The mathematical expressions then become more elaborate since they involve the mixing and quenching cross sections as well as the optical transition probabilities for each of the two excitation levels (see Jenkins[34]).

The expressions given also become useless when optical transitions to or from the ground level are allowed for only one of the fine-structure levels. This case applies for the ^2D-doublets of Tl, of which only the $^2D_{\frac{3}{2}}$ level is optically connected to the $6^2P_{\frac{1}{2}}$ ground level.

REFERENCES

[1] J. D. Winefordner, M. L. Parsons, J. M. Mansfield and W. J. McCarthy, *Analyt. Chem.* **39**, 436 (1967).

[2] D. R. Jenkins, *Spectrochim. Acta*, **23B**, 167 (1967).

[3] H. P. Hooymayers, 'Quenching of excited alkali atoms and hydroxyl radicals and related effects in flames'. *Ph.D. Thesis*. Utrecht (1966).

P.A.C.—23/1—H

[4] H. P. Hooymayers and C. Th. J. Alkemade, *J. Quant. Spectr. Radiative Transfer*, **6**, 501 (1966).
[5] C. Th. J. Alkemade and P. J. Th. Zeegers, in J. D. Winefordner (Ed.), *Spectrochemical Methods of Analysis* (Interscience Series 'Advances in Analytical Chemistry and Instrumentation'), Part I, Chapter 1, In preparation.
[6] R. Mavrodineanu and H. Boiteux, *Flame Spectroscopy*. Wiley: New York (1965).
[7] H. P. Hooymayers and C. Th. J. Alkemade, *J. Quant. Spectr. Radiative Transfer*, **6**, 847 (1966).
[8] D. R. Jenkins, *Proc. Roy. Soc. A*, **293**, 493 (1966).
[9] J. M. Mansfield, M. P. Bratzel, H. O. Norgordon, D. O. Knapp, K. E. Zacha and J. D. Winefordner, *Spectrochim. Acta*, **23B**, 389 (1968).
[10] H. Prugger, *Spectrochim. Acta*, **24B**, 197 (1969).
[11] D. R. Jenkins· *Proc. Roy. Soc. A*, **306**, 413 (1968).
[12] D. R. Jenkins, *Proc. Roy. Soc. A*, **303**, 453 (1968).
[13] D. R. Jenkins, *Proc. Roy. Soc. A*., **303**, 467 (1968).
[14] H. P. Hooymayers and G. Nienhuis, *J. Quant. Spectr. Radiative Transfer*, **8**, 955 (1968).
[15] H. P. Hooymayers and P. L. Lijnse, *J. Quant. Spectr. Radiative Transfer*, **9**, 995 (1969).
[16] S. J. Pearce, L. de Galan and J. D. Winefordner, *Spectrochim. Acta*, **23B**, 793 (1968).
[17] P. J. Th. Zeegers and J. D. Winefordner, submitted to *Spectrochim. Acta*.
[18] W. J. McCarthy, M. L. Parsons and J. D. Winefordner, *Spectrochim. Acta*, **23B**, 25 (1967).
[19] C. Th. J. Alkemade, *Tenth International Spectroscopy Colloquium*, p 143. (College Park, Maryland, 1962). Spartan Books: Washington (1963).
[20] C. Th. J. Alkemade, *Appl. Optics*, **7**, 1261 (1968).
[21] J. D. Winefordner and J. M. Mansfield, *Appl. Spectrosc. Revs*, **1**, 1 (1967).
[22] J. D. Winefordner, M. L. Parsons, J. M. Mansfield and W. J. McCarthy, *Spectrochim. Acta*, **23B**, 37 (1967).
[23] H. P. Hooymayers, *Spectrochim. Acta*, **23B**, 567 (1968).
[24] P. J. Th. Zeegers, R. Smith and J. D. Winefordner, *Analyt. Chem.* **40**, 26A (1968).
[25] B. H. Armstrong, *J. Quant. Spectr. Radiative Transfer*, **7**, 61 (1967).
[26] C. Young, *Rep. ORA–05863*, University of Michigan: Ann Arbor (1965).
[27] C. van Trigt, T. Hollander and C. Th. J. Alkemade, *J. Quant. Spectr. Radiative Transfer*, **5**, 813 (1965).
[28] R. Herrmann and C. Th. J. Alkemade, *Chemical Analysis by Flame Photometry* (translated by P. T. Gilbert). Interscience: New York (1963).
[29] A. C. G. Mitchell and M. W. Zemansky, 'Resonance radiation and excited atoms, 1' reprint. Cambridge University Press: London (1961).
[30] L. de Galan, W. W. McGee and J. D. Winefordner, *Analyt. Chim. Acta*, **37**, 436 (1967).
[31] C. Veillon, J. M. Mansfield and M. L. Parsons, *Analyt. Chem.* **38**, 204 (1966).
[32] P. Pringsheim, *Fluorescence and Phosphorescence*. Interscience: New York (1949).
[33] N. Omenetto and G. Rossi, *Spectrochim. Acta*, **24B**, 95 (1969).
[34] D. R. Jenkins, *Trans. Faraday Soc.* **64**, 36 (1968).